

Rate-Flexible Coherent PON Up To 300 Gb/s Demonstrations with Low Complexity TDM Burst Design

Haipeng Zhang, Zhensheng Jia, Luis Alberto Campos, and Curtis Knittle

Cable Television Laboratories Inc., 858 Coal Creek Circle, Louisville, CO 80027.

h.zhang@cablelabs.com; s.jia@cablelabs.com

Abstract: Two flexible-rate coherent PON architectures have been demonstrated, featuring a low complexity TDM burst DSP. A peak data rate of up to 300-Gb/s and transmission over 50-km link and 1×32 split ratio has been achieved. © 2023 The Author(s)

1. Introduction

Passive optical network (PON) based on a point-to-multipoint topology has been widely deployed worldwide over the last two decades and has become the dominant solution to meet the ever-increasing capacity requirements in the optical access networks [1-5]. The development of PON technology over the past 20 years has been primarily focused on intensity modulation / direct detection (IM/DD) and has followed two families of standards: ITU-T Question 2/Study Group 15 (Q2/15) and IEEE 802.3 Ethernet working group [1, 3], as shown in Fig. 1(a). On the way to the next generation 100 Gb/s and beyond PON, existing IM/DD solutions suffer from limited power budget, bandwidth limitation, and transmission impairments such as chromatic dispersion and are considered too challenging [1, 4]. Coherent optical technology on the other hand, is a breakthrough solution because of its superior performance and enormous potential in terms of high receiver sensitivity and powerful digital equalization capabilities against fiber link impairment [1, 4, 5]. Recently, the industry has started to establish the working group to develop a set of foundational specifications for single-wavelength coherent PON towards 100 Gb/s and beyond.

Existing PON typically has a static configuration in physical layer, meaning that a certain peak capacity is specified by the worst performing ONU with limited flexibility and non-optimal resource allocation [6, 7]. In contrast, the future generation PON aims to be flexible by offering adaptive capacity and link budget to meet end-user requirements [6, 7]. Coherent PON leverages the high capacity of coherent optics, a large link budget for extended coverage, and a high split ratio, providing capabilities to adaptively allocate network resources and optimize capacity based on end-user's locations and needs. Fig. 1(b) shows a conceptual scheme for a rate-flexible coherent PON that uses multiple modulation formats with different link budget to serve customers in different locations, resulting in efficient resource usage, improved performance, and overall architectural flexibility.

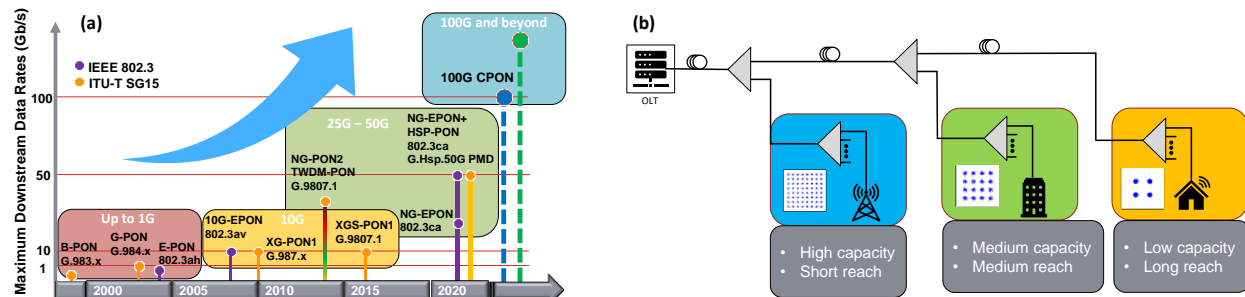


Fig. 1. (a) PON evolution; (b) concept of flexible rate coherent PON.

In this work, we propose a simple flexible data rate time division multiplexing (TDM) burst-based design that features burst receiver digital signal processing (DSP) with low complexity, without the need for a complicated modulation format identification algorithm. We experimentally demonstrate two novel coherent PON architectures with flexible data rate, one features comb-based multiple wavelengths for downstream broadcasting and TDM burst with three modulation formats for upstream, and the other uses TDM with three modulation formats for downstream and burst frame upstream. A peak data rate of up to 300 Gb/s and transmission over 50 km of fiber optic link and a split ratio of 1×32 have been achieved.

2. Operating Principles

The overall digital signal processing (DSP) procedures with the proposed modulation format identification associated with the corresponding coherent TDM burst demodulation algorithms for the upstream are plotted in Fig. 2(a). Three modulation formats are considered here as an example: dual-polarization quadrature phase shift keying (DP-QPSK), dual-polarization 16 quadrature amplitude modulation (DP-16QAM), and dual-polarization 64 quadrature amplitude modulation (DP-64QAM). Finer granularity in net information rate can be generated by adopting probabilistic constellation shaping (PCS) and adaptive forward error correction (FEC) coding for future

work. First, a burst frame identification algorithm based on power detection is implemented to locate each burst frame. In this step, the burst frame size is calculated from the identified burst. This is then followed by chromatic dispersion (CD) compensation, burst clock recovery and synchronization. Detailed information in coherent burst preamble design can be found in [1, 4]. After burst signal reception, the payload signals are processed by conventional first-stage coherent DSP. Note that the three modulation formats share the same burst reception and first-stage DSP up to the constant modulus algorithm (CMA), after that DP-16QAM and DP-64QAM are processed with additional K-means and Gaussian mixture model (GMM) algorithms to improve the performance of multi-modulus algorithm (MMA) and carrier phase estimation (CPE) [8]. Burst frame size obtained from the first step is used to make decisions after the CMA, since each modulation format is assigned a different burst frame length.

Fig. 2(b) shows burst frame design examples for the three modulation formats mentioned above. On top, a burst frame with 102.4 ns preamble and 921.6 ns payload is assigned to a 25-GBd DP-QPSK signal for data rate of 100 Gb/s. In the middle, a frame design with the same preamble and a longer 1.946 μ s payload uses a 25-GBd DP-16QAM signal to target a 200 Gb/s data rate. At the bottom, a longest frame with 3.994 μ s payload is driven by a 25-GBd DP-64QAM signal targeting a data rate of 300 Gb/s. In the design, the three burst frame designs have the same preamble length, and all preambles use the DP-QPSK modulation format to ensure robust burst signal detection. Note that the burst frame designs in Fig. 2(b) are examples for the experimental demonstration, for actual deployment any modulation format can be assigned to a range of frame sizes, as long as these frame sets can be distinguished from other frame designs that are assigned with other modulation formats.

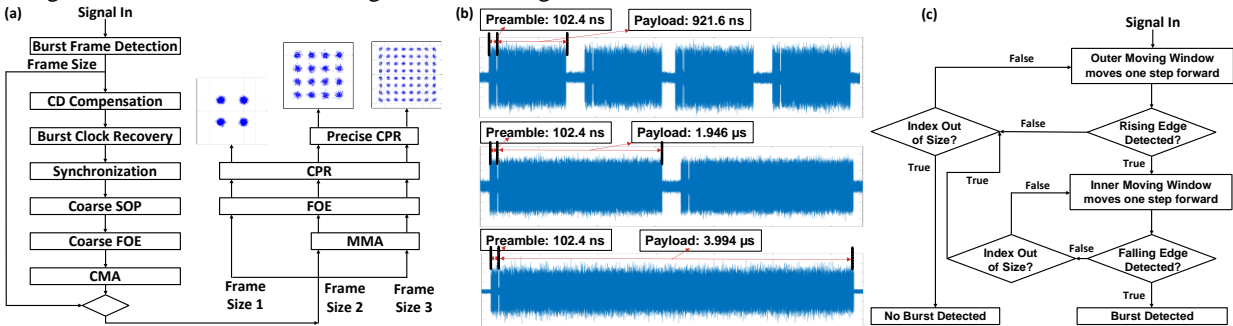


Fig. 2. (a) Proposed DSP processes with burst frame detection for modulation format identification; (b) burst frame design examples; (c) burst frame detection procedures.

Fig. 2(c) shows detailed procedures of the power-based burst frame detection process. First the received data stream is smoothed to produce a binary map that uses ‘0’s to represent signal components below a preset threshold and ‘1’s to represent signal components above the threshold. A burst frame boundary search is then performed by locating the abrupt changes on the binary map. After finding rising and falling edges, a burst frame is located, and its length is estimated based on the edges. This process is not requiring a fast Fourier transform since the data stream is processed in the time domain.

3. Experimental Setup and Results

Leverage the flexible rate TDM burst design, we propose two coherent PON architectures offering the data rates at 100 Gb/s, 200Gb/s, and 300Gb/s. The scheme of the first proposed coherent PON link is shown in Fig. 3(a). In this architecture, both downstream (DS) and upstream (US) signals are generated by coherent driver modulators (CDMs) using 25-GBd DP-QPSK, DP-16QAM, and DP-64QAM signals and transmitted in the TDM burst, with each data rate being assigned a specific frame length to support different rates simultaneously.

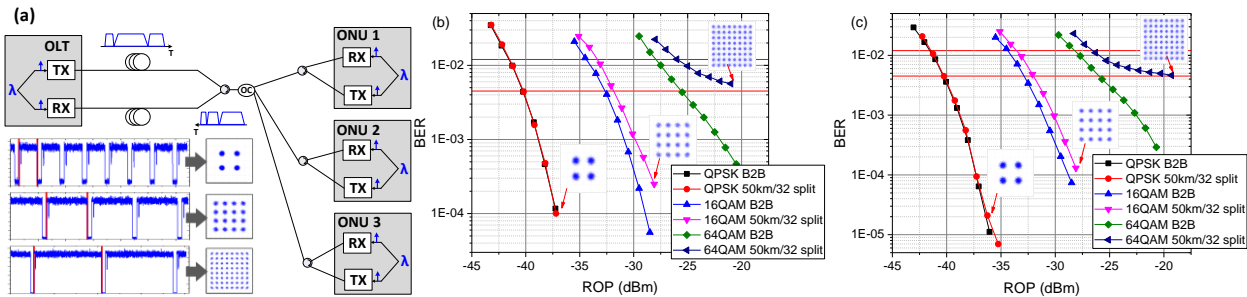


Fig. 3. (a) Rate flexible coherent PON setup with TDM burst DS and US; (b) BER versus ROP for DS signal transmission; (c) BER versus ROP for US signal transmission.

The inset of Fig. 3(a) shows detected burst frames carrying different modulation formats using the proposed burst frame detection, with red markers indicating the start and end of the detected burst. In this design only one wavelength is used for both transmission directions to minimize hardware complexity and costs, especially in the ONUs. The optical distribution network (ODN) consists of two 50 km fiber links and a 1×32 passive optical splitter. The two-fiber design is adopted to route the DS and US signals to mitigate penalties due to reflections in the link [9]. This design can take advantage of the use cases where fiber is abundant and redundant fiber links have been deployed. And as a result, each ONU requires only one laser, which can be fixed wavelength, which can significantly reduce the cost of equipment at the customer site, which is the most sensitive element in the PON. Fig. 3(b) and Fig. 3(c) show bit-error-rate (BER) performance versus the received optical power (ROP) for DS and US transmission respectively. For reference, back-to-back (B2B) BER vs. ROP results, along with staircase hard-decision (HD) FEC threshold at $\text{BER}=4.5\text{E-}3$ and concatenated soft decision (SD) FEC threshold at $\text{BER}=1.2\text{E-}2$, are included in both diagrams. The system functionality of the proposed architecture has been verified experimentally through bidirectional transmission with the TDM scheme. Benefiting from the two-fiber link, no significant performance degradation due to reflections in the link has been observed for different data rates.

The second proposed architecture uses time and wavelength division multiplexing (TWDM) over a single fiber link as shown in Fig. 4(a). In this configuration, DS signals are sent at three different data rates (100 Gb/s, 200 Gb/s, and 300 Gb/s) in continuous mode. Where the US signal is transmitted in TDM burst. On the OLT side, four optical tones (λ_1 : 1563.46nm, λ_2 : 1563.86nm, λ_3 : 1564.26nm, λ_4 : 1564.66nm) are generated via an optical frequency comb generated from an external cavity laser and cascaded electro-optic modulators. The first three tones (λ_1 - λ_3) are fed into CDMs to generate DS signals using 25-Gb/s DP-QPSK, DP-16QAM, and DP-64QAM modulation formats, respectively. The fourth tone (λ_4) is sent into an optical injection locking (OIL) setup consisting of a polarization controller (PC), an optical circulator, and a Fabry-Perot laser diode (FP-LD). The output of the OIL setup is used as a local oscillator (LO) for US signal detection. The ODN consists of a 50 km fiber link and a 1×32 optical splitter. On the ONU side, each ONU can choose the DS signal data rate by adjusting its LO wavelength. Meanwhile, for US transmission the specific TDM frame length is now assigned to each modulation format. Rate-flexible PON operation is achieved by selecting the DS wavelength and the US TDM frame length.

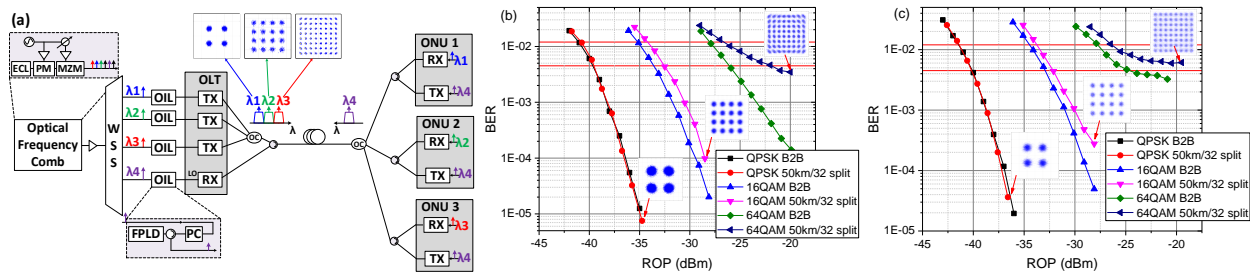


Fig. 4. (a) Rate flexible coherent PON setup with broadcast DS and TDM burst US; (b) BER versus ROP for DS signal transmission; (c) BER versus ROP for US signal transmission.

Fig. 4(b) shows BER performance versus ROP for DS transmission. The first three wavelengths (λ_1 , λ_2 , and λ_3) from the OFC source carry 25-Gb/s DP-QPSK, 25-Gb/s DP-16QAM, and 25-Gb/s DP-64QAM signals respectively. OIL lasers are used in the OLT transmitters. On the ONU side, LO wavelengths are tuned to match the three DS wavelengths to receive desired DS signals. Similarly, the TDM US transmission BER versus ROP results are shown in Fig. 4(c). For US signal detection, OIL laser is used as LO in OLT receiver. For reference, B2B BER vs. ROP results, along with staircase HD FEC and concatenated SD FEC threshold, are included in both charts.

4. Conclusion

In this work, we propose two coherent PON architectures with a low complexity flexible data rate design from different modulation format for next-generation coherent PON at 100 Gb/s, 200Gb/s, and 300Gb/s data rates. Two flexible data rate network architectures are experimentally demonstrated over 50-km fiber transmission and 1×32 passive splitting with one using comb-based multiple wavelengths for downstream broadcast and TDM burst for upstream and the other using TDM burst for downstream and upstream. The proposed coherent PON schemes show superior flexibility to serve different applications with different requirements of data rate, link budget, range, latency, etc. for the future ultra-high capacity optical access networks.

Reference

- [1]. J. Zhang, et al., *J. Opt. Commun. Netw.*, 13(2), A135-A143 (2021).
- [2]. D. van Veen and V. Houtsma, *Proc. OFC 2017*, paper Th5A.4.
- [3]. V. Houtsma et al., *Proc. OFC 2019* paper M2B.1.
- [4]. J. Zhang, et al., *Proc. OFC 2020*, paper W1E.1.
- [5]. R. Matsumoto, et al., *Proc. OFC 2018*, paper M3B.2.
- [6]. S. Xing, et al., *Proc. OFC 2022*, paper Th4A.4.
- [7]. V. Houtsma, et al., *J. Light Technol.*, 38.12, 3261-3267(2020).
- [8]. M. Xu, et al., *Proc. OFC 2019*, paper M2H.1.
- [9]. H. Zhang, et al., *Proc. OFC 2022*, paper M11.5.